Lung vessel segmentation in CT images using graph-cuts

Zhiwei Zhai, Marius Staring, and Berend C. Stoel

Division of Image Processing, Department of Radiology, Leiden University Medical Center, Leiden, The Netherlands

ABSTRACT

Accurate lung vessel segmentation is an important operation for lung CT analysis. Filters that are based on analyzing the eigenvalues of the Hessian matrix are popular for pulmonary vessel enhancement. However, due to their low response at vessel bifurcations and vessel boundaries, extracting lung vessels by thresholding the vesselness is not sufficiently accurate. Some methods turn to graph-cuts for more accurate segmentation, as it incorporates neighbourhood information. In this work, we propose a new graph-cuts cost function combining appearance and shape, where CT intensity represents appearance and vesselness from a Hessian-based filter represents shape. Due to the amount of voxels in high resolution CT scans, the memory requirement and time consumption for building a graph structure is very high. In order to make the graph representation computationally tractable, those voxels that are considered clearly background are removed from the graph nodes, using a threshold on the vesselness map. The graph structure is then established based on the remaining voxel nodes, source/sink nodes and the neighbourhood relationship of the remaining voxels. Vessels are segmented by minimizing the energy cost function with the graph-cuts optimization framework. We optimized the parameters used in the graph-cuts cost function and evaluated the proposed method with two manually labeled sub-volumes. For independent evaluation, we used 20 CT scans of the VESSEL12 challenge. The evaluation results of the sub-volume data show that the proposed method produced a more accurate vessel segmentation compared to the previous methods, with F1 score 0.76 and 0.69. In the VESSEL12 data-set, our method obtained a competitive performance with an area under the ROC curve of 0.975, especially among the binary submissions.

Keywords: Graph-cuts, vessel segmentation, vesselness, appearance and shape

1. INTRODUCTION

Lung vessel detection is a key research topic in pulmonary CT image processing, since accurate vessel segmentation is an important step in extracting imaging bio-markers of vascular lung diseases. For example, systemic sclerosis (SSc) is related to pulmonary hypertension (PH),[1] which is related to narrowing of the small vessels, and therefore vessel analysis could be used as an imaging bio-marker for PH analysis in SSc. A few methods have been proposed for lung vessel segmentation. According to the VESSEL12 challenge,[2] Hessian-based methods are popular and perform well in lung vessel enhancement. Hessian-based filters, such as the Frangi filter[3] and Sato filter,[4] enhance tube-like structures by modeling the eigenvalues of the Hessian matrix with cylindrical properties. However, these filters tend to give a low response at the vessel bifurcations and at the vessel boundaries. In our previous work, a strain energy filter[5] overcomes the problem in detecting bifurcations to some degree by analyzing the shape-tuned strain energy density. However, thresholding the strain energy filter's vesselness does not provide accurate binary results either. In order to improve vessel segmentation, we turn to graph-cuts where we can more easily combine different sources of information via the cost function, and additionally include neighboring information.

Graph-cuts methods consider the segmentation a labeling problem.[6–8] The voxel nodes are labeled to object or background, according to nodes neighbor connections and their weights.[9] Several approaches using graph-cuts for vessel segmentation have been proposed. Chen et al.[10] proposed a regional graph-cuts based method for liver vessel segmentation with quick shift clustering for initialization. Bauer et al.[11] proposed a tube detection filter for a rough vessel segmentation, then the shape prior from centerline and radius of the initial vessel trees

Further author information:
E-mail: z.zhai@lumc.nl, Telephone: +31 71 52 66967

were used to constrain the graph-cuts. Freiman et al.[12] proposed a graph-cuts based method for carotid artery segmentation by coupling Frangi's vesselness and intensity into cost function. In order to cope with memory and computational challenges, they divided the scan volume into several block regions with a small overlap, computed graph-cuts for each block independently, and merged the binary segmentations results.

In this paper, an automatic lung vessel segmentation method is proposed based on graph-cuts. The Hessian-based strain energy filter is adopted to enhance vessels. A conservative threshold is applied on the vesselness to label voxels that are certainly part of the background, the remaining voxels are included as nodes in the graph. Instead of using vesselness as the vessel data cost term directly,[12] we take it as a shape feature and compute the vessel data term with prior distribution. CT intensity represents appearance. Combining appearance and shape, the cost function is calculated. To deal with memory requirements of graph structure representations, we removed those voxel nodes that are considered clearly background and employed a low overhead sparse matrix implementation to record the remaining voxel nodes neighborhood connections and their weights. After the graph structure is established, the graph-cuts optimization framework is applied for vessel segmentation. The proposed lung vessel segmentation method was optimized and evaluated on two manually labeled sub-volumes and evaluated independently on the VESSEL12 challenge data-set.

2. METHODS

Our segmentation method consists of three steps: 1) application of the strain energy filter for lung vessels enhancement, 2) construction of the graph structure representation, and 3) vessels segmentation based on graph-cuts.

2.1 Vessel enhancement filter

The response of traditional Hessian-based vesselness filters is low at the vessel bifurcations and boundaries, due to an overly simplified cylindrical model. The strain energy filter, which is based on strain energy density theory from solid mechanics, aims to remedy this. The Hessian matrix is considered a stress tensor, and three tensor invariants (measures) can be derived from orthogonal tensor decomposition, each measuring an independent descriptor of material distortion. Turning to images, they can be used to formulate distinctive functions for shape discrimination, brightness contrast and structure strength. Based on an intensity continuity assumption, and a relative Hessian strength measure to ensure the dominance of second-order over first-order derivatives to suppress undesired step edges, the final vesselness was calculated as follow:

$$\varphi(\sigma, x) = \begin{cases} 0, & \text{if } \frac{1}{3}(\lambda_1 + \lambda_2 + \lambda_3) > -\zeta\lambda_m \\ \exp\left(-\eta\frac{||\nabla I||}{\lambda_m}\right) V^{\kappa}(x)\rho(H, v), & \text{otherwise,} \end{cases} \tag{1}$$

in which σ is scale, λ_i are the eigenvalues with λ_m the maximum eigenvalue, $\lambda_1 + \lambda_2 + \lambda_3$ is the brightness contrast term, $\frac{||\nabla I||}{\lambda_m}$ measures relative Hessian strength, $V^{\kappa}(x)$ is a measure for vessel shape and $\rho(H, v)$ measures structure strength. The parameters $0 < \zeta < 1, \eta > 0, \kappa > 0$ and $-1 < v < 0.5$ are user-defined. More details can be found in the original paper.[5]

2.2 Graph representation

For high resolution pulmonary CT scans, there are around 500 slices per patient with 512*512 voxels per slice. Even when only considering the lung region for computing, the graph would consist of almost ten million nodes and hundred million edges (26-connectivity in a 3D grid). To cope with memory requirements, previous works used a block region strategy.[10,12] However, this introduces discontinuities in the merged part of detected vessel. Therefore we used an alternative method to reduce the graph size by a thresholding strategy. As illustrated in Figure 1a, there are several voxels with lowest gray values that are certainly part of the background. Then, we can use a low threshold to label these voxels as background, see Figure 1b. The graph structure can be established using the remaining voxels (unlabeled voxels).

In Figure 1c, the nodes of the graph consist of the remaining voxels, source and sink nodes. The edges between the source/sink node and voxel nodes are called t-edges and the edges between neighboring voxel nodes

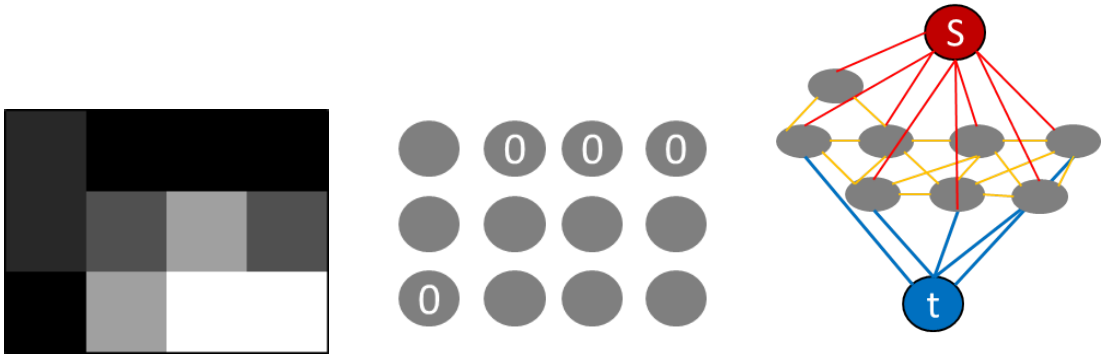

(a) (b) (c)

Figure 1: Graph structure representation of this method, (a) original image, (b) pre-labeling the background with the threshold strategy, (c) graph structure construction of the remaining voxel nodes.

are n-edges. The t-edges and their weights can be represented easily with a dense matrix. For the n-edges, a sparse matrix was adopted to record the adjacent connections and their weights. If we use 1 and 0 to represent the relationship 'adjacency' and 'non-adjacency' of the voxels respectively, all the 1s locate in several diagonals of the sparse adjacency matrix. The sparse adjacency matrix can be determined memory efficiently by assigning the diagonal vectors. The diagonal vectors can be generated easily by analyzing the type of adjacency. Then, the n-edge's adjacency matrix can be extracted from the whole 3D grid sparse adjacency matrix with the remaining voxels' indices.

To illustrate the sparse adjacency matrix analysis method, we take a 3 by 4 2D image as an example and only consider 4-connectedness. For 4-connectedness, there are only two types of adjacency (if considering adjacency with direction, there would be four types of adjacency), up-down adjacency and left-right adjacency, see Figure 2b. Taking the up to down adjacency, the sparse matrix can be generated efficiently by assigning the single diagonal with one vector. The vector can be determined by a rule that the $(k \times 3)$th element is zero. The left to right adjacency sparse matrix can be calculated in a similar way. After combining these two sparse adjacency matrices, and making the combined matrix symmetric, so that the down to up adjacency and right to left adjacency are included, we obtain the final sparse adjacency matrix, Figure 2c. For a 3D image, the calculation of a sparse adjacency matrix is similar.

2.3 Proposed cost function for the graph-cuts

In this work, we present a method for lung vessel segmentation based on graph-cuts, by combining appearance and shape features. Segmentation is treated as a labeling problem, solved by graph-cuts $L = \{L_p | p \in \mathcal{P}\}$. The energy function of a labeling problem can be optimized by finding the max-flow/min-cut algorithms.[7] The energy function of our method is:

$$E(L) = \sum_{p \in \mathcal{P}} \left(w D_p^{CT}(L_p) + (1-w) D_p^{vsl}(L_p) \right) + \gamma \sum_{(p,q) \in \mathcal{N}, L_p \neq L_q} V_{p,q}(L_p, L_q), \tag{2}$$

where the data term consists of appearance (CT intensity) $D_p^{CT}(L_p)$ and shape (vesselness) $D_p^{vsl}(L_p))$ and w is a weight balancing the two parts. $V_{p,q}(L_p, L_q)$ is the cost function for cutting the edge (p, q) and γ is a user-defined positive coefficient for adjusting the smoothness.

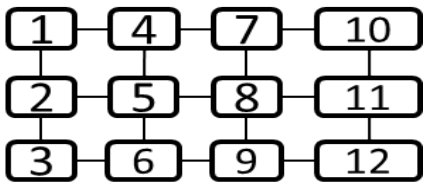

(a)

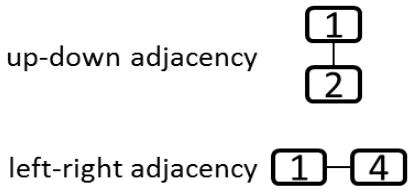

(b)

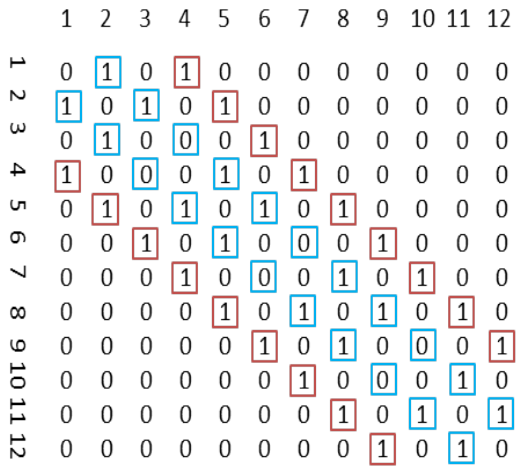

(c)

Figure 2: 2D image sparse adjacency matrix, (a) is a 3 by 4 2D matrix with the value of the voxel index inside, (b) is the adjacency type analysis, (c) is the sparse adjacency matrix of the 2D image.

Commonly Gaussian functions are used in the data term,[12] but this would cause voxels with high intensity or vesselness, i.e. far away from the center of the Gaussian distribution, to obtain a low vessel probability. Therefore we employed a sigmoid function for both the appearance term and the shape term. So, voxels with high a intensity or vesselness obtain a high vessel likelihood, as follows:

$$D_p^{CT}(I_p|L_p = l) = \frac{1}{1 + e^{-\alpha_l^{CT}(I_p - \beta_l^{CT})}} \tag{3}$$

$$D_p^{vsl}(I_p|L_p = l) = \frac{1}{1 + e^{-\alpha_l^{vsl}(I_p - \beta_l^{vsl})}}. \tag{4}$$

The choice for the free parameters of the sigmoid function in Equation (3) and (4), is given in Sec. 3.1. The cost function $V_{p,q}(L_p, L_q)$ for the n-edge (p, q) is calculated based on the similarity in appearance of two voxels nodes p q, and weighted by their spatial distance:

$$V_{p,q}(L_p, L_q) = \begin{cases} e^{-\frac{|I_p - I_q|}{dist(p,q)}}, & \text{if } L_p \neq L_q \quad \text{and} \quad (p,q) \in \mathcal{N} \\ 0, & \text{otherwise} \end{cases} \tag{5}$$

If two nodes of the n-edge (p, q) have similar appearance but are labeled differently, the boundary cost of this n-edge will be high, weighted by the spatial distance of nodes p and q.

3. EXPERIMENTS AND RESULTS

This work were implemented in Matlab for the graph structure construction and mixed with C++ for the cost function optimization, which is benefiting from GCmex 1.9 (http://www.wisdom.weizmann.ac.il/~bagon/matlab_code/GCmex1.9.tar.gz). The source code of the vessel enhancement filters is publicly available via the toolkit ITKTools (https://github.com/ITKTools/ITKTools), see the tool pxenhancement. The entire processing pipeline was designed in MeVisLab 2.7.1 (VC12-64). The runtime of the proposed method for a typical $400 \times 512 \times 512$ size 3D CT image is around 650s on our computer, configured with a 2.67 GHz CPU, 24 GB memory and a 64-bit Windows 7 operating system.

Table 1: Evaluation results of methods on reference standard data sets

		Data1			Data2		
Enhancement	binarization	Recall	Precision	F1 score	Recall	Precision	F1 score
Frangi[3]	threshold	0.7344	0.5082	0.6007	0.6285	0.5147	0.5660
Freiman's method[12]	graph-cuts	0.8233	0.4781	0.6048	0.6428	0.4868	0.5541
Strain energy[5]	threshold	0.7082	0.7287	0.7183	0.6223	0.7119	0.6641
Strain energy	graph-cuts	0.7331	0.7917	0.7613	0.6673	0.7145	0.6901

3.1 Parameter estimation

The parameters used in the strain energy vesselness filter were set according to the literature:[5] $\zeta = 0.5$, $\eta = \kappa = 0.2$, $v = 0.0$, and using scales $\sigma \in \{1, 2, 3\}$. After construction of the graph structure, the parameters in the graph-cuts energy function were trained with sub-volume data which was labeled by an expert. More details about the sub-volume data can be found in Sec. 3.2. Due to the complex structure of the vessel trees, the smoothness parameter γ was set to 0.01. After optimizing on the training data, the appearance and shape balance parameter w in the data term was set to 0.6. For the parameters of the sigmoid function in the data term, we designed an algorithm to estimate them automatically. Before estimation, we removed voxels that had high vesselness or intensity, because these voxels can affect the parameters estimation severely. Afterwards, the mean value was taken as the initial threshold to separate the initial background and foreground. The Gaussian distribution of the intensity of the foreground can be estimated by calculating the mean μ and the standard deviation std. Then, we fitted the sigmoid function to the Gaussian function in the way that $Sigmoid(\beta) = Gaussian(\beta) = 0.5$. For estimating the fuzziness parameter α we did several experiments and finally found that the best fitting curve was obtained by: $Sigmoid(\mu) = 0.95$. So, all the parameters used in the sigmoid function for the foreground intensity term are estimated, and the parameters used in the cost function for the vesselness term can be calculated similarly.

3.2 Data and results

Clinical image data was acquired of two patients on a Toshiba Aquilion 16 detector row CT scanner without contrast media. Due to the complexity of the pulmonary vessel trees, it is unrealistic to manually extract the entire vessel trees. In order to evaluate the proposed lung vessel segmentation method, we chose two sub-volumes on the boundary of pulmonary lobes, where the bright plane-shaped fissure and plenty of vessel details make it a challenging detection task. Subsequently, a technical expert and a pulmonologist were asked to manually label the data, using the interactive tools of ITK-snap.[13] In total, two reference segmentations, Data1 with size 65*60*120 and Data2 with size 91*70*121, were extracted. The original CT and extracted sub-volume region of Data1 is shown in Figure 3.

Centerline-based evaluation was applied to these two sub-volumes. The vessel centerlines were extracted from the binary masks using a skeletonization method based on the distance transform.[14] As shown in Figure 4, the centerline of the segmentation result was compared with the centerline of the reference standard. If the distance between the voxels on the two centerlines are less than the vessel radius at that point, i.e. the voxels on the segmentation centerline fall inside the reference standard vessel region, they would be counted as true positive. The number of false negatives was calculated by the number of voxels on the reference standard centerline minus the number of true positives. The number of false positives was calculated using the number of voxels on segmented centerlines minus the number of true positives, i.e. the number of voxels falls outside the vessel regions of the reference standard. The $precision = TP/(TP + FP)$ and $recall = TP/(TP + FN)$ were calculated, and the $F1$ score, $2\frac{precision*recall}{precision+recall}$, was taken as the main evaluation measurement. We compared the performance of the proposed graph-cuts vessel segmentation method with the result from thresholding the Frangi's vesselness,[3] thresholding the strain energy filter's vesselness[5] and the Freiman's based method.[12] For the optimization of the threshold-based vesselness methods, 70 thresholds ranging from the minimum to the maximum vesselness were used and the best evaluation result was selected. For the Freiman's based method, we implemented the method according to the literature[12] and optimized the parameters with the sub-volume Data1. The evaluation results are shown in Table 1. According to the evaluation results, our proposed method achieved a better segmentation.

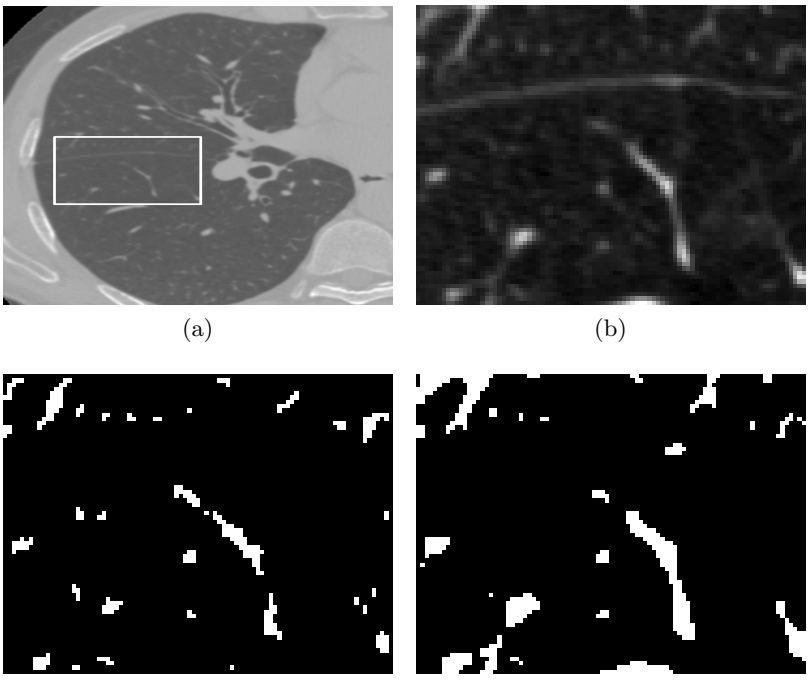

(a) (b) (c) (d)

Figure 3: Segmentation result on a reference region, (a) reference region in the CT, (b) one slice of the extracted region, (c) manually segmented reference standard, (d) segmentation result of the proposed method.

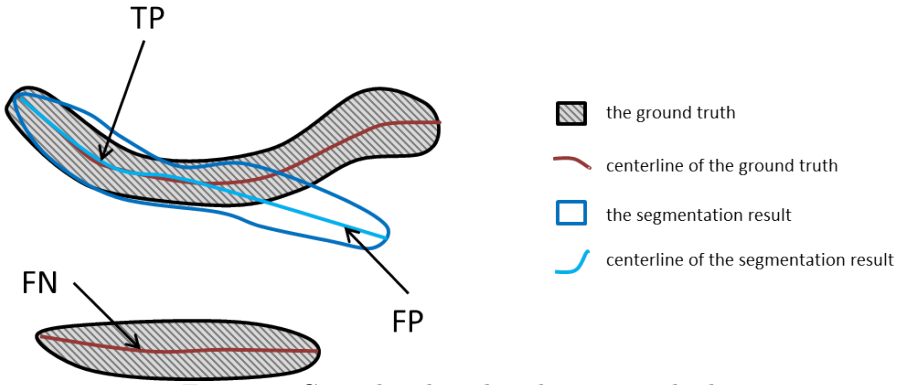

Figure 4: Centerline-based evaluation method.

For an independent evaluation, we used the VESSEL12 challenge data-set, which consists of 20 anonymized CT scans from three hospitals:[2] University Medical Center Utrecht, the University Clinic of Navarra and Radboud University Nijmegen Medical Center. The scans have been selected such that in approximately half of the scans contrast agent was used. About half of the scans contained abnormalities such as nodules, emphysema or pulmonary embolisms. The CT scan size was around 512*512*400, with voxel size around $0.7*0.7*0.7mm^3$. This represents a variety of CT scanner types and image acquisition settings, and a wide range of clinical images. The scan data and lung masks were provided by the organizers. The manual labeling was performed on pre-generated points, and only those points were kept when the labels from three independent observers were the same. There were nine categories in the reference standard to perform a comprehensive evaluation of vessel segmentation. The vessel segmentation result from the participating algorithms were evaluated against the manually annotations.

For our study, we downloaded the CT scans and lung mask data, we applied the graph-cuts vessel segmentation, after shape feature extracting with the strain energy filter. We submitted our binary segmentation results

Table 2: Evaluation results of the VESSEL12 data-set: Az score, Specificity and Sensitivity of our submission across all categories. (Categories 1: Principal, 2: Small Vessels, 3: Medium Vessels, 4: Large Vessels, 5: Vessel/Airway Wall, 6: Vessel/Dense Lesion, 7: Vessel/Mucus-filled bronchi, 8: Vessel-in-lesion/Lesion, 9: Vessel/Nodules).

	1	2	3	4	5	6	7	8	9
Az	0.975	0.953	0.977	0.993	0.867	0.481	0.331	0.661	0.238
Specificity	0.910	0.865	0.910	0.979	0.588	0.239	0.112	0.451	0.038
Sensitivity	0.929	0.966	0.953	0.960	0.929	0.929	0.929	0.829	0.929

to the VESSEL12 organizers, and the organizers made the independent evaluation and sent the evaluation results to us. Our method obtained an area under the ROC curve (Az) of 0.975 score, which is a competitive performance on VESSEL12, especially among the binary submissions. The evaluation results of our method is shown in Table 2. The evaluation results of the other submissions can be found in the VESSEL12 study paper[2] and the VESSEL12 website http://vessel12.grand-challenge.org.

4. CONCLUSION AND DISCUSSION

A graph-cuts based segmentation method was proposed to extract the pulmonary vessels in thoracic CT images. By combining appearance and shape features, a new cost function was designed. An efficient strategy was adopted to cope with the memory requirements of a graph representation. We performed training and evaluation with own sub-volume data, and independently evaluated our method with the VESSEL12 challenge data. From the evaluation results, the proposed method obtained a competitive performance.

From the results on the in-house data, see Table 1, the F1 score of our method was higher than the threshold-based vesselness methods and the Freiman's based method. The performance of strain energy filter was better than Frangi's filter, which has been reported in literature,[5] and we reproduced the previous results. The Freiman's based method was not a lot better than the threshold-based Frangi's method. This is likely caused by the fact that the Freiman's based method uses a Gaussian as a cost function. This means that high intensity and vesselness values produce low vessel likelihood, which may cause under-segmentation. Additionally, the Freiman's based method does not use a parameter to balance between appearance and shape features. In our method, we designed a new cost function in the graph-cuts for vessels segmentation, which is better than the threshold-based strain energy method. In general, the graph-cuts could perform better than the thresholding, but one should be careful with designing this, since the graph-cuts may give poorer results by a suboptimal choice of cost function (as seen in Data2 in Table 1). From the results on the VESSEL12 data (Table 2), the proposed method obtained a good performance on the overall categories 1-4. However, the segmentation method did not perform very well in distinguishing airway walls from vessels (category 5), because some airway walls had similar intensities as vessels and parts of the airway walls were attached to the pulmonary artery. The lower score in category 7 was caused by mucus-filled bronchi that have similar appearance and shape features as vessels. To compensate for this, a separate algorithm would be needed for detecting the bronchial tree and extending this tree by mucus-filled bronchi, to be used as an exclusion method. Because in categories 6, 8 and 9, lesions and nodules are mostly attached to vessel trees, the graph-cuts method was not able to separate them from vessel trees. For the other participating methods in the VESSEL12, distinguishing these bronchi, lesions and nodules were also challenges for pulmonary vessel segmentation. Comparing with the other submissions, we obtained a competitive score, which was the highest compared to the other binary submissions. This method could be improved by combining more information in the data term, such as a distance map to vessel centerlines of initial segmentation, and designing a more precise boundary cost function with multiple features.

Acknowledgment

We would like to thank the VESSEL12 Challenge organizers for the data collection and the ground-truth labels. We also thank Jan Stolk for supplying the in-house data, and Denis Shamonin, Yuchuan Qiao, Zhuo Sun and Hessam Sokooti for exchanging ideas. This work is supported by the China Scholarship Council No.201406120046.

REFERENCES

1. E. Hachulla, V. Gressin, L. Guillevin, *et al.*, "Early detection of pulmonary arterial hypertension in systemic sclerosis: a French nationwide prospective multicenter study," *Arthritis & Rheumatism* **52**(12), pp. 3792–3800, 2005.
2. R. D. Rudyanto, S. Kerkstra, E. M. Van Rikxoort, *et al.*, "Comparing algorithms for automated vessel segmentation in computed tomography scans of the lung: the VESSEL12 study," *Medical image analysis* **18**(7), pp. 1217–1232, 2014.
3. A. F. Frangi, W. J. Niessen, K. L. Vincken, and M. A. Viergever, "Multiscale vessel enhancement filtering," in *Medical Image Computing and Computer-Assisted Interventation*, pp. 130–137, Springer, 1998.
4. Y. Sato, S. Nakajima, N. Shiraga, H. Atsumi, S. Yoshida, T. Koller, G. Gerig, and R. Kikinis, "Three-dimensional multi-scale line filter for segmentation and visualization of curvilinear structures in medical images," *Medical image analysis* **2**(2), pp. 143–168, 1998.
5. C. Xiao, M. Staring, D. Shamonin, J. H. Reiber, J. Stolk, and B. C. Stoel, "A strain energy filter for 3D vessel enhancement with application to pulmonary CT images," *Medical image analysis* **15**(1), pp. 112–124, 2011.
6. Y. Boykov and V. Kolmogorov, "An experimental comparison of min-cut/max-flow algorithms for energy minimization in vision," in *Energy minimization methods in computer vision and pattern recognition*, pp. 359–374, Springer, 2001.
7. Y. Y. Boykov and M.-P. Jolly, "Interactive graph cuts for optimal boundary & region segmentation of objects in nd images," in *Computer Vision, 2001. ICCV 2001. Proceedings. Eighth IEEE International Conference on*, **1**, pp. 105–112, IEEE, 2001.
8. Y. Boykov, O. Veksler, and R. Zabih, "Fast approximate energy minimization via graph cuts," *Pattern Analysis and Machine Intelligence, IEEE Transactions on* **23**(11), pp. 1222–1239, 2001.
9. M. B. Salah, A. Mitiche, and I. B. Ayed, "Multiregion image segmentation by parametric kernel graph cuts," *Image Processing, IEEE Transactions on* **20**(2), pp. 545–557, 2011.
10. B. Chen, Y. Sun, and S. H. Ong, "Liver vessel segmentation using graph cuts with quick shift initialization," in *The 15th International Conference on Biomedical Engineering*, pp. 188–191, Springer, 2014.
11. C. Bauer, T. Pock, E. Sorantin, H. Bischof, and R. Beichel, "Segmentation of interwoven 3d tubular tree structures utilizing shape priors and graph cuts," *Medical image analysis* **14**(2), pp. 172–184, 2010.
12. M. Freiman, N. Broide, M. Natanzon, *et al.*, "Vessels-cut: a graph based approach to patient-specific carotid arteries modeling," in *Modelling the Physiological Human*, pp. 1–12, Springer, 2009.
13. P. A. Yushkevich, J. Piven, H. C. Hazlett, R. G. Smith, S. Ho, J. C. Gee, and G. Gerig, "User-guided 3d active contour segmentation of anatomical structures: significantly improved efficiency and reliability," *Neuroimage* **31**(3), pp. 1116–1128, 2006.
14. D. Selle, B. Preim, A. Schenk, and H.-O. Peitgen, "Analysis of vasculature for liver surgical planning," *Medical Imaging, IEEE Transactions on* **21**(11), pp. 1344–1357, 2002.